Critical Review

Structural Studies of G Protein-Coupled Receptors

Mengjie Lu[1,2]
Beili Wu[1,3]*

[1]*CAS Key laboratory of Receptor Research, Shanghai Institute of Materia Medica, Chinese Academy of Sciences, Shanghai, China*
[2]*University of Chinese Academy of Sciences, Beijing, China*
[3]*School of Life Science and Technology, ShanghaiTech University, Pudong, Shanghai, China*

Abstract

G protein-coupled receptors (GPCRs) comprise the largest membrane protein family. These receptors sense a variety of signaling molecules, activate multiple intracellular signal pathways, and act as the targets of over 40% of marketed drugs. Recent progress on GPCR structural studies provides invaluable insights into the structure–function relationship of the GPCR superfamily, deepening our understanding about the molecular mechanisms of GPCR signal transduction. Here, we review recent breakthroughs on GPCR structure determination and the structural features of GPCRs, and take the structures of chemokine receptor CCR5 and purinergic receptors $P2Y_1R$ and $P2Y_{12}R$ as examples to discuss the importance of GPCR structures on functional studies and drug discovery. In addition, we discuss the prospect of GPCR structure-based drug discovery. © 2016 IUBMB Life, 68(11):894–903, 2016

Keywords: *G protein-coupled receptor; structural studies; chemokine receptor; purinergic receptor*

Introduction

Over 800 GPCRs have been identified in human cells (as shown in the IUPHAR website: http://www.guidetopharmacology.org/GRAC/FamilyDisplayForward?familyId=694&familyType=GPCR). Based on their sequence similarities and pharmacological properties, human GPCRs are grouped into four subfamilies: rhodopsin-like receptors (class A), secretin and adhesion receptors (class B), glutamate receptors (class C), and frizzled/taste2 receptors (class F; (1–3)). These receptors are activated by a wide spectrum of extracellular stimuli, including photons, ions, neurotransmitters, lipids, chemokines, and hormones, and then couple to G proteins and initiate downstream signaling networks, resulting in a broad range of physiological and pathological processes (4). GPCRs are involved in numerous human diseases and represent the largest drug target protein family. Over 40% of marketed drugs target GPCRs and are used to treat many human diseases, such as central nervous system disorders, inflammatory diseases, metabolic imbalances, cardiac diseases, and cancer etc (5,6). However, there still remains enormous potential for GPCR drug development (5). Structural information of GPCRs is urgently needed to better understand the molecular mechanisms of cell signaling and develop new drugs for the treatment of severe human diseases.

Volume 68, Number 11, November 2016, Pages 894–903
Address correspondence to: Beili Wu, CAS Key laboratory of Receptor Research, Shanghai Institute of Materia Medica, Chinese Academy of Sciences, 555 Zuchongzhi Road, Shanghai 201203, China.
Tel: ++86-21-2023-9065.
E-mail: beiliwu@simm.ac.cn
Received 12 August 2016; Accepted 8 October 2016
DOI 10.1002/iub.1578
Published online 20 October 2016 in Wiley Online Library (wileyonlinelibrary.com)

Structure Determination of GPCRs

Structural studies of GPCRs remain enormously difficult due to low protein expression level in native tissues and heterologous systems, poor protein stability and multiple conformational states of the receptors (7). In recent years, new methods and technologies in membrane protein engineering and crystallization have been developed to facilitate GPCR structure determination. To improve the receptor stability and provide more polar surface for forming crystal lattice contacts, fusion partners, such as T4 lysozyme, thermo-stabilized apocytochrome

b562RIL and rubredoxin etc, are inserted into the flexible regions of the receptor, usually the third intracellular loop and N-terminus (8). Alanine scanning mutagenesis (9) and engineering disulfide bridges (10) were also used to stabilize the conformation of GPCRs. Adding ligands with high selectivity and high binding affinity or antibodies during protein purification and crystallization help to lock the receptor in a single conformational state (11,12), which is required by successful crystallization and structure determination. *In meso* crystallization approaches in which protein samples are diffused into the lipidic cubic phase (LCP) were utilized to solve most of the GPCR structures (13). Using LCP for crystallization is essential as it mimics favorable environment for membrane proteins and allows for easy addition of sterols and other lipid-like molecules to facilitate crystallization. Very recently, the development of X-ray free-electron laser (XFEL) greatly raised the possibility of obtaining high-resolution diffraction data from micrometer- and submicrometer size crystals (14).

With the application of these new techniques, methods and strategies, there was an exponential growth of GPCR structures. To date, more than 130 structures have been solved (Table 1). These structures provide unprecedented insights into GPCR structure–function relationship. Next, we will review structural features of GPCRs, and discuss the molecular mechanisms of GPCR-ligand interaction and receptor activation.

Structural Features of GPCRs

The GPCR structures share a similar overall architecture that consists of a canonical seven transmembrane (7TM) α-helical bundle (helices I–VII) with N-terminus and three extracellular loops (ECL1-3) at the extracellular side, and C-terminus and three intracellular loops (ICL1-3) at the intracellular side. Although GPCRs are diverse in sequence and length, the solved structures show similarities, indicating similar mechanisms of signal transduction that GPCRs may share. Meanwhile, different GPCR structures reveal distinct structural features, which provide molecular basis of recognizing various ligands by different receptors.

Extracellular Region

Three extracellular loops of GPCRs play important roles on shaping the entrance to the ligand-binding pockets. The longest extracellular loop, ECL2, exhibits distinct conformation in different GPCR structures, but similar structural features for the members within a same subfamily. It forms an α-helical structure in the adrenergic receptor structures, and a β-hairpin in the structures of peptide receptors. In most of the known GPCR structures, ECL2 is anchored to the extracellular tip of helix III by a highly conserved disulfide bond between $Cys^{3.25}$ and Cys^{ECL2}, which limits the movement of ECL2 and stabilizes the conformation of the extracellular region (4). Compared with ECL2, ECL1 and ECL3 are relatively short and often lack secondary structures. The extracellular regions of GPCRs exhibit two different types of conformation, occluding the ligand-binding pocket or leaving the binding pocket water accessible, to modulate the ligand access and binding (Fig. 1).

7TM Region

The 7TM regions of GPCRs play important roles in signal transduction. In comparing the inactive and active structures of β_2AR, M_2R and μ-OR, a large outward shift of helix VI and smaller movements of helices V and VII at the intracellular side of the receptors have been observed, demonstrating that the rearrangement of the cytoplasmic parts of helices V, VI and VII plays a critical role in the process of GPCR activation ((15–17); Fig. 2A,C). In addition, large movements of the extracellular ends of helices VI and VII have been observed in the agonist-bound structures of $P2Y_{12}R$ compared with its antagonist-bound structure, indicating that the conformational changes at the extracellular side of the receptor are also involved in GPCR activation ((18); Fig. 2B,D).

Despite the similar 7TM helical architecture, the transmembrane regions of different GPCRs form diverse ligand-binding pockets varying in size, shape and electrostatics, providing structural basis for recognizing various ligands. The ligand-binding pockets of GPCRs bound to small-molecule endogenous ligands, such as aminergic and nucleotide receptors, are relatively small and deep within the 7TM helical bundle. In contrast, the binding pockets of peptide receptors are larger and more open, and closer to the extracellular surface, while the binding pockets in the structures of lipid receptors are covered by the N-terminus and extracellular loops to make the pockets more hydrophobic (Fig. 3A).

Based on the locations of their binding sites compared to the binding sites of the endogenous ligands, GPCR ligands are divided into orthosteric ligands and allosteric modulators. The binding sites of the orthosteric ligands are usually within the 7TM helical bundle and close to the extracellular surface. However, the locations of the allosteric ligand-binding sites are less conserved. In the M_2R structure, the positive allosteric modulator LY2119620 locates at the extracellular region and situates above the orthosteric site ((16); Fig. 3B). In contrast, the allosteric ligand-binding sites locate deeper in the 7TM region than the orthosteric sites in the structures of CCR5 and CRF_1R ((19,20); Fig. 3C). Recently, unexpected allosteric ligand-binding sites located entirely outside of the helical bundle have been observed in the structures of $P2Y_1R$ and the 7TM domain of GCGR ((21,22); Fig. 3D), greatly extending our knowledge about the mechanisms of GPCR ligand recognition. Allosteric modulators have been suggested to potentially provide more selective and/or effective therapies than the orthosteric ligands as the allosteric ligand-binding sites are much less conserved than the orthosteric ligand-binding sites (23). Elucidation of the structural details of allosteric ligand-binding sites will accelerate the process of structure-based drug discovery.

Intracellular Region

Once signals are transduced from the 7TM region to the intracellular part of the receptor, residues in the intracellular region interact with signaling effectors, such as G proteins,

TABLE 1 ***Solved crystal structures of GPCRs***

Receptor type		*Receptor*	*Number of structures*	*References*
Class A GPCRs		Rhodopsin	30	(10,27,49,50)
	Aminergic receptors	β_2AR	16	(15,33,51)
		β_1AR	17	(32,52)
		H_1R	1	(53)
		D_3R	1	(54)
		5-HT_{1B}	2	(55)
		5-HT_{2B}	2	(14,56)
		M_1R	1	(57)
		M_2R	3	(16,58)
		M_3R	4	(59)
		M_4R	1	(57)
	Nucleotide receptors	A_{2A}AR	14	(60,61)
		$P2Y_{12}$R	3	(18,28)
		$P2Y_1$R	2	(21)
	Peptide receptors	CXCR4	6	(31,62)
		CCR5	1	(19)
		NOP	1	(63)
		κ-OR	1	(64)
		μ-OR	2	(17,65)
		δ-OR	4	(24)
		NTSR1	5	(66)
		PAR1	1	(67)
		OX_2R	2	(68)
		AT_1R	2	(69)
	Lipid receptors	$S1P_1$	2	(70)
		FFAR1	1	(71)
		LPA_1	3	(72)
Class B GPCRs		GCGR	2	(22,73)
		CRF_1R	1	(20)
Class C GPCRs		$mGluR_1$	1	(74)
		$mGluR_5$	3	(75)
Class F GPCR		SMO	6	(76)

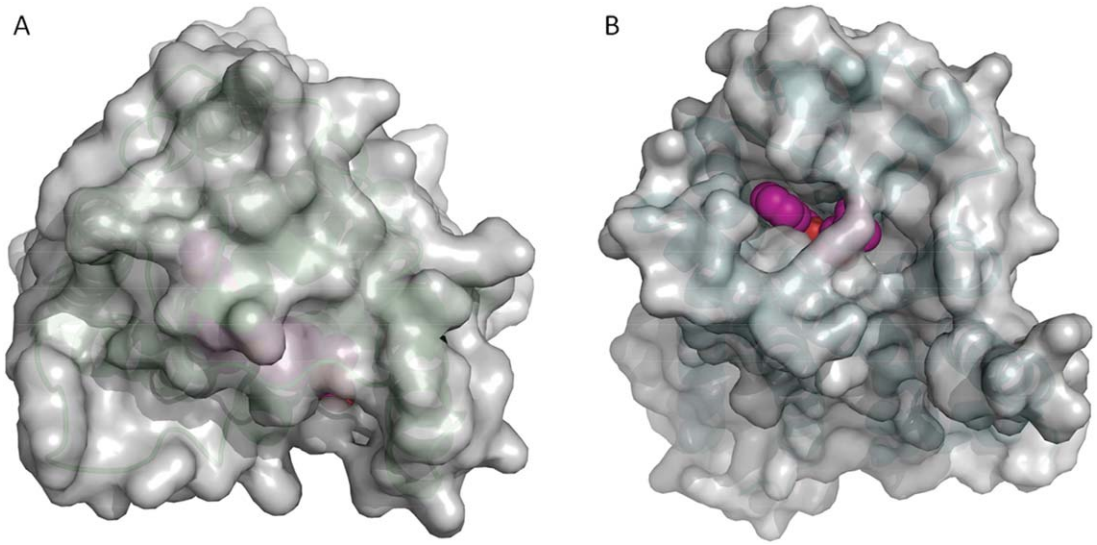

FIG 1 *Conformations of the extracellular regions in the structures of LPA_1 (A) and β_2AR (B). The structures of LPA_1 (PDB ID: 4Z36) and β_2AR (PDB ID: 2RH1) are shown as cartoon and surface representations. Ligands are shown as spheres and colored in magenta.*

GPCR kinases and arrestins, to initiate downstream signal pathways. In the known GPCR structures, ICLs exhibit either short α-helical structures or unstructured stretch. A fully resolved of ICL3 was observed in the high-resolution structure of the human δ-OR bound to an antagonist naltrindole, showing that ICL3 adopts a "closed" conformation, which stabilizes the conformation of helices V and VI and may play a role in hindering the receptor activation (24). A short intracellular helix VIII running parallel to the membrane surface was observed in most of the GPCR structures. Helix VIII has been reported to be involved in receptor activation and plays important roles in interacting with multiple signaling effectors (25,26). In the structure of β_2AR in complex with Gs protein, the C terminus of the Gα subunit interacts with the intracellular parts of helices III, V, and VI as well as ICL2 (*15*). The rhodopsin-arrestin complex structure reveals an interface formed by the intracellular parts of helices V, VI, and VII, the N terminus of helix VIII, and ICL1-3 of rhodopsin (27).

Structures of Chemokine Receptor CCR5 and Purinergic Receptors $P2Y_1R$ and $P2Y_{12}R$

In recent years, we successfully solved crystal structures of three GPCRs, including chemokine receptor CCR5 (*19*), and purinergic receptors $P2Y_{12}R$ (18,28) and $P2Y_1R$ (21). These structures provide molecular details of ligand-binding landscape of these three receptors, and deepen our understanding about the GPCR signaling mechanisms.

Chemokine Receptor CCR5

Chemokines and their receptors play key roles in immune responses and inflammation. The chemokine family consists of about 50 members that bind to 20 chemokine receptors (29). The complexity and diversity of chemokine-chemokine receptor interactions relate to pathogenesis and outcome of numerous human diseases. Chemokine receptors CCR5 and CXCR4 act as two co-receptors of human immunodeficiency virus type 1 (HIV-1) to facilitate viral entry by interacting with the viral envelope glycoprotein gp120 (30). HIV-1 can infect a variety of immune cells by changing its co-receptor specificity. In 2013, we determined the complex structure of CCR5 bound to an HIV entry inhibitor maraviroc, providing insights into the mechanisms of allosteric inhibition of chemokine signaling and viral entry by maraviroc and HIV-1 coreceptor selectivity (19).

Maraviroc was reported as an allosteric modulator of CCR5, but its allosteric mechanism remained unclear. The N-terminus and ECL2 of CCR5 have been identified as the major recognition sites of HIV-1 gp120 and chemokine ligands. The CCR5-maraviroc complex structure reveals a ligand-binding site of maraviroc buried within the 7TM helical bundle of the receptor (Fig. 4A), making no contacts with the N-terminus or ECL2, which indicates that maraviroc can not inhibit HIV-1 infection or chemokine signaling by causing spatial hindrance like the orthosteric ligands. In the CCR5 structure, we found that maraviroc behaved as an inverse agonist and stabilized the conformation of the receptor in an inactive state. The conformations of two highly conserved class A GPCR residues $Trp248^{6.48}$ and $Tyr244^{6.44}$, which are considered to be involved in GPCR activation, are similar to those observed in other inactive GPCR structures but distinct from their active-state conformations. Additionally, the ligand maraviroc forms a strong interaction with the residue $Trp248^{6.48}$ to prevent its activation-related conformational change, further stabilizing the inactive conformation of CCR5. The above structural information suggests that maraviroc most likely blocks HIV-1 viral

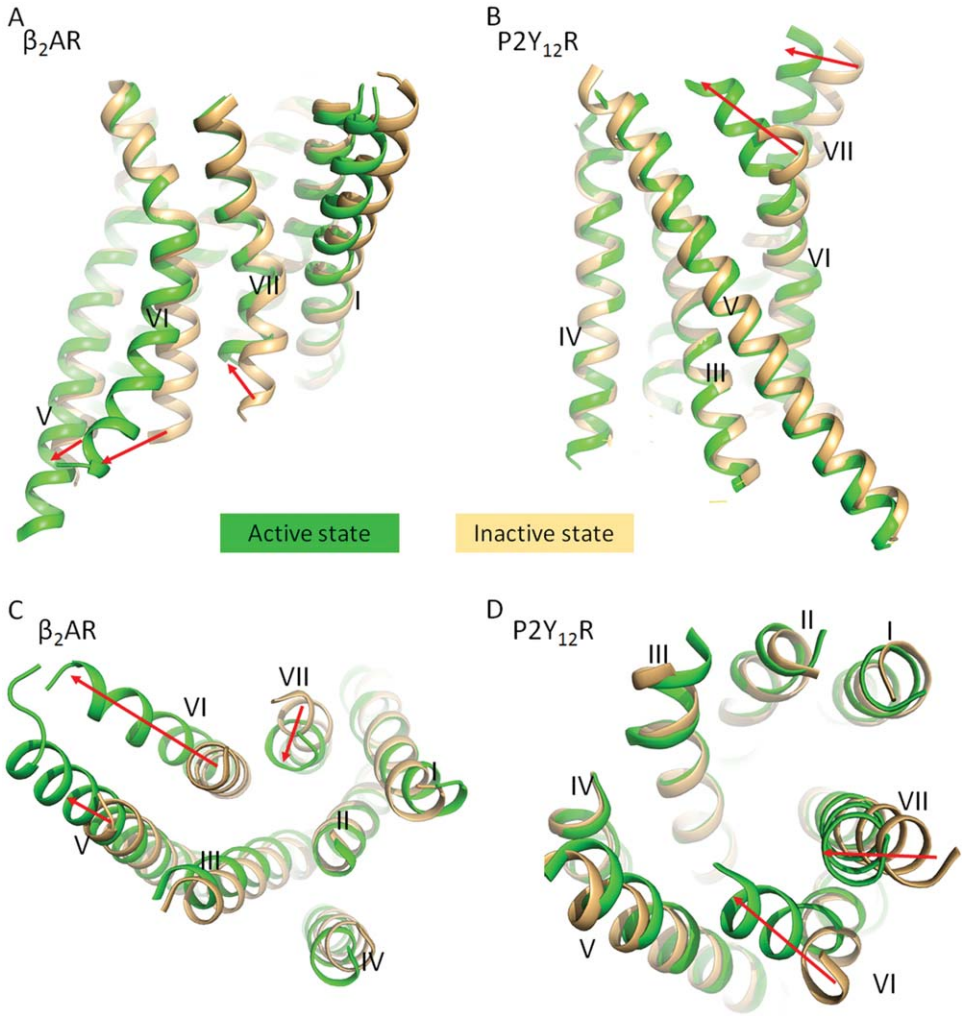

FIG 2 *Comparison of the active and inactive structures of β_2AR and P2Y$_{12}$R. A and C: Side and cytoplasmic views of the β_2AR-Gs complex structure (PDB ID: 3SN6, green) and the structure of β_2AR bound to the antagonist carazolol (PDB ID: 2RH1, wheat). B and D: Side and top views of the P2Y$_{12}$R-2MeSADP (PDB ID: 4PXZ, green) and P2Y$_{12}$R-AZD1283 (PDB ID: 4NTJ, wheat) structures. The structures of the 7TM helical bundles of β_2AR and P2Y$_{12}$R are shown in cartoon representation. Movements of the helices are shown by arrows.*

entry and chemokine binding in an allosteric inverse agonism manner by locking the CCR5 conformation in an inactive state.

Comparing the CCR5 structure with the previously solved structure of CXCR4 (*31*), substantial differences have been found. In CCR5, a short intracellular helix VIII is observed, while the C-terminal region adopts an extended disordered conformation in the CXCR4 structure. Helix IV in CCR5 is tilted by about 15° compared with the corresponding helix in CXCR4, and its intracellular portion is shorter than in CXCR4. More importantly, we found the ligand-binding pockets of these two co-receptors varied in size, shape, and electrostatics. In the CXCR4 structure, due to the shift of helix VII and ECL2, the entrance to the ligand-binding pocket is partially covered by its N-terminus and ECL2, while the ligand-binding pocket of CCR5 is more open. The binding site for maraviroc in CCR5 is deeper, and extends toward helices V and VI, occupying a larger area at the bottom of the pocket compared to the binding site of IT1t in CXCR4. And for the charge distribution, the CXCR4 ligand-binding pocket is more negatively charged than the binding pocket in CCR5. These structural differences could be determinants of HIV-1 co-receptor selectivity. The third variable region, V3 loop, of the HIV-1 gp120 has been identified as the major determinant of co-receptor specificity. Sequence analysis and mutagenesis studies have found that the V3 region is more positively charged in the X4-tropic viruses (using CXCR4 as the co-receptor) than the R5-tropic viruses (using CCR5 as the co-receptor).This is correlated with the fact that CXCR4 ligand-binding pocket is more negatively charged. Our models of the complexes between CCR5/CXCR4 and the V3 loops further support that charge distributions and steric hindrances caused by residue substitutions in the ligand-binding pockets of the co-receptors may be major determinants of HIV-1 co-receptor selectivity.

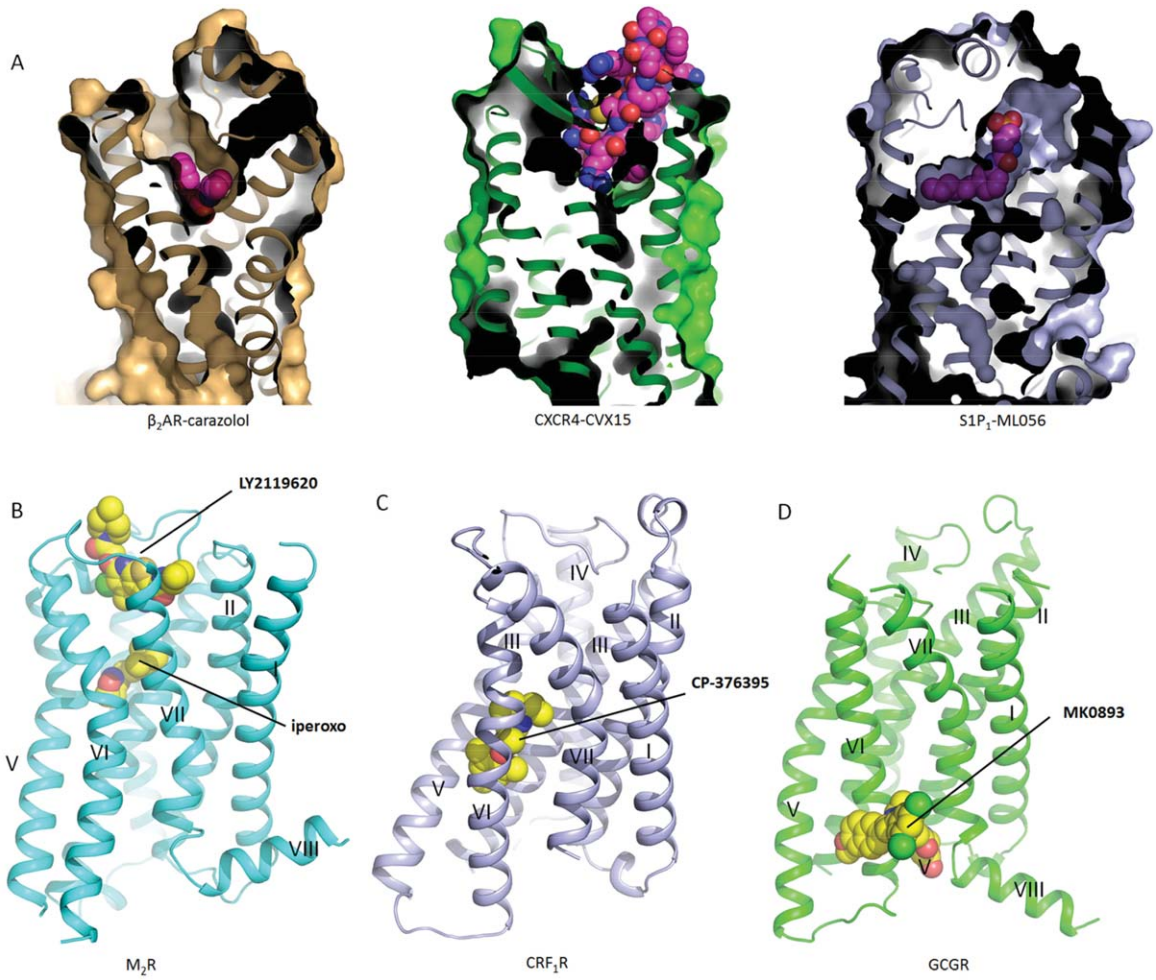

FIG 3

Different locations of ligand-binding sites in GPCRs. A: The ligand-binding pockets in the complexes structures of β_2AR-carazolol (PDB ID: 2RH1), CXCR4-CVX15 (PDB ID: 3OE0), and S1P$_1$-ML056 (PDB ID: 3V2Y). The receptors are shown in cartoon and surface presentations (β_2AR: orange; CXCR4: green; S1P$_1$: blue). The ligands are displayed as magenta spheres. B: The structure of M$_2$R bound to the orthosteric agonist iperoxo and the allosteric positive allosteric modulator LY2119620 (PDB ID: 4MQT). C: The structure of CRF$_1$R bound to the allosteric antagonist CP-376395 (PDB ID: 4K5Y). D: The structure of GCGR's 7TM domain bound to the allosteric antagonist MK0893 (PDB ID: 5EE7). The receptors are shown in cartoon (M$_2$R: cyan; CRF$_1$R: blue; GCGR: green). Ligands are shown as yellow spheres.

Purinergic Receptor P2Y$_{12}$R

Purinergic receptors P2Y$_1$R and P2Y$_{12}$R play important roles in platelet aggregation, which make them attractive antithrombotic drug targets. In 2014, we solved three structures of P2Y$_{12}$R in complex with an antagonist AZD1283 and two agonists 2MeSADP and 2MeSATP (18,28). Recently, we determined the complex structures of P2Y$_1$R bound to a nucleotide-like antagonist MRS2500 and a non-nucleotide antagonist BPTU (21).

The P2Y$_{12}$R structures reveal some structural features that set it apart from the other GPCR structures. Due to lack of the conserved residue P$^{5.50}$, helix V of P2Y$_{12}$R adopts a straight conformation that is different from most of the other solved class A GPCR structures. Another feature is that the P2Y$_{12}$R-AZD1283 complex structure lacks the highly conserved disulfide bond between Cys$^{3.25}$ and Cys^{ECL2}, which is observed in most of GPCR structures. However, with substantial conformational changes in helix III and helix V, this disulfide bond is clearly observed in the agonist-bound structure, suggesting that this conserved disulfide bond not only serves for the stabilization of 7TM helical scaffold, but also potentially plays a role in regulation of receptor activation and signal transduction.

A very striking observation in the P2Y$_{12}$R structures is that two potential ligand-binding pockets may simultaneously exist in the receptor. The agonist 2MeSADP and the antagonist AZD1283 occupy one of the pockets, while the other one remains available, suggesting that P2Y$_{12}$R may simultaneously bind to two different ligands. Docking simulation data suggest that the active metabolites of some P2Y$_{12}$R drugs may occupy the second pocket and behave as allosteric regulators of the receptor. In addition, simulation data suggest that the

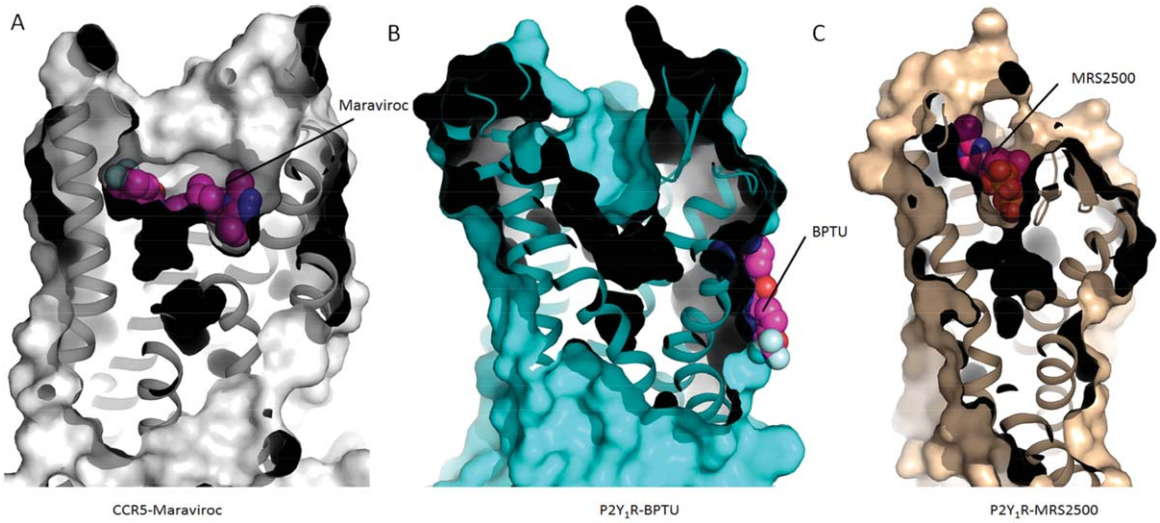

FIG 4 *Ligand-binding pockets of maraviroc in CCR5 (A), and BPTU and MRS2500 in $P2Y_1R$ (B and C). The receptors (PDB ID: 4MBS, 4XNV and 4XNW) are shown in cartoon and surface representations and the ligands are shown in magenta sphere representation.*

endogenous ligand ADP can also bind to this allosteric site and serves as an inhibitor of the receptor. This two-site model provides essential insights for the development of new $P2Y_{12}R$ drugs for the treatment of thrombosis.

GPCRs transduce the extracellular signals to the intracellular signaling effectors by adopting conformational changes. Previous GPCR structural studies suggested that the conformational changes mainly occured in the intracellular region during receptor activation. However, comparing the agonist- and antagonist-bound structures of $P2Y_{12}R$, large conformational movements were observed in the extracellular region. Upon binding to the agonist, the extracellular tips of helices VI and VII shift over 10 and 5 Å, respectively, toward the central axis of the 7TM helical bundle. This is the first example, to our knowledge, of a GPCR in which the large rearrangement of the extracellular region is required for receptor activation.

Purinergic Receptor $P2Y_1R$

The most striking information observed in the $P2Y_1R$ structures is that the nucleotide-like antagonist MRS2500 and the non-nucleotide antagonist BPTU occupy two completely different ligand-binding sites (Fig. 4B,C). The binding site of MRS2500 locates within the 7TM helical bundle and is closer to the extracellular surface than the small-molecule ligand-binding sites in the other known GPCR structures. Although $P2Y_1R$ and $P2Y_{12}R$ recognize the same endogenous ligand, adenosine 5′-diphosphate (ADP), the binding modes of these two purinergic receptors to their nucleotide-like ligands observed in the complex structures of $P2Y_1R$-MRS2500 and $P2Y_{12}R$-2MeSADP are very different with spatially distinct ligand-binding sites, which slightly overlap at phosphate binding regions. The orientations of the two ligands are also different. The adenine ring of MRS2500 is adjacent to helices VI and VII in the $P2Y_1R$ structure, and the adenine group of 2MeSADP reaches deep into the bindng pocket and interacts with helices III and IV in $P2Y_{12}R$. These structural differences highlight the diversity of GPCR signal recognition mechanisms.

Surprisingly, the non-nucleotide antagonist BPTU binds to an allosteric pocket on the external, lipid-exposed receptor surface, suggesting that this highly hydrophobic ligand may access to its binding pocket through the lipid bilayer. Our ligand-binding assay showed that BPTU allosterically modulated the receptor function by accelerating the dissociation of the agonist 2MeSADP. BPTU is the first structurally characterized selective GPCR ligand that locates entirely outside of the canonical GPCR ligand-binding pocket, greatly extending our knowledge about the ligand-binding modes of GPCRs.

The $P2Y_1R$ structures provide insights into the inhibition mechanisms of MRS2500 and BPTU. Previous GPCR structural studies demonstrated that the conformational changes of helices V–VII played major roles in receptor activation. The binding mode of MRS2500 in $P2Y_1R$ indicates that this antagonist most likely inhibits receptor function by preventing the movements of helices VI and VII. However, BPTU can not take the same approach as it makes no contacts with helices V, VI, and VII. The BPTU-bound $P2Y_1R$ structure suggests that this ligand may inhibit receptor activation by blocking the conformational changes of helices II and III, possibly a rotation of helix III, which was also reported to be involved in the activation of some GPCRs (32–34), although it is very subtle. The above findings imply that the movements of both domains, helices I–IV and helices V–VII, of GPCRs are equally important for receptor activation.

GPCR Structure-Based Drug Discovery

GPCRs serve as targets of about 40% of approved drugs, but <20% of GPCRs have been targeted (35). High-throughput

screening (HTS) is currently the most commonly used strategy to identify novel ligands for GPCRs (36). However, this approach is always expensive and time consuming. Structure-based approach has become widely used as a drug discovery tool since 1990s (37,38). But it resulted in limited successes in GPCR drug discovery before GPCR structures became available (38), as the predicted homology models were not able to provide accurate structural information to guide rational drug design. The recent progress on GPCR structural studies has facilitated the drug discovery of GPCRs. In 2012, Mysinger et al. reported their studies on structure-based virtual screening of CXCR4 ligands using a protein homology model and the crystal structure of CXCR4. The results indicated that the crystal structure had significant advantages, showing a considerably higher hit rate, over the homology model (39). In 2009, Kolb et al. used this approach to screen a library of about one million compounds against the crystal structure of β_2AR and many novel chemotypes and scaffolds with high binding affinity were identified (40). A similar approach was applied to A_{2A}AR (41), H_1R (42), D_3R (43), M_2R and M_3R (44), 5-HT_{1B} and 5-HT_{2B} (45) to identify novel ligand scaffolds. Hit rates were significantly higher compared to that in HTS in most cases.

In recent years, the phenomena that biased ligands and GPCR dimerization affect receptor pharmacology and signaling have added new dimensions to drug discovery (46–48). However, the available GPCR structures are insufficient to investigate the structural basis for biased signaling and receptor dimerization, or further yield novel drugs through the structure-based approach. More GPCR structures are urgently needed to develop better GPCR drugs with better specificity and pharmacodynamics.

Conclusions

The recent progress on GPCR structural studies deepens our understanding about the structure-function relationship of GPCRs. In this review, we discussed the structural features of the solved GPCR structures, which provide insights into the molecular mechanisms of GPCR signal recognition, transduction and modulation. However, the current structural information is insufficient. More high-resolution structures of different GPCRs are still required to fully understand the physiological behaviors of the GPCR superfamily and facilitate structure-based drug discovery for the treatment of many severe human diseases.

References

[1] Lagerstrom, M. C., and Schioth, H. B. (2008) Structural diversity of G protein-coupled receptors and significance for drug discovery. Nat. Rev. Drug Discov. 7, 339–357.

[2] Kolakowski, L. F. Jr. (1994) GCRDb: a G-protein-coupled receptor database. Receptors & Channels 2, 1–7.

[3] Fredriksson, R., Lagerstrom, M. C., Lundin, L. G., and Schioth, H. B. (2003) The G-protein-coupled receptors in the human genome form five main families. Phylogenetic analysis, paralogon groups, and fingerprints. Mol. Pharmacol. 63, 1256–1272.

[4] Venkatakrishnan, A. J., Deupi, X., Lebon, G., Tate, C. G., Schertler, G. F., et al. (2013) Molecular signatures of G-protein-coupled receptors. Nature 494, 185–194.

[5] Schlyer, S., and Horuk, R. (2006) I want a new drug: G-protein-coupled receptors in drug development. Drug Discov. Today 11, 481–493.

[6] Thomsen, W., Frazer, J., and Unett, D. (2005) Functional assays for screening GPCR targets. Curr. Opin. Biotechnol. 16, 655–665.

[7] Zhao, Q., and Wu, B. (2012) Ice breaking in GPCR structural biology. Acta Pharmacol. Sin. 33, 324–334.

[8] Chun, E., Thompson, A. A., Liu, W., Roth, C. B., Griffith, M. T., et al. (2012) Fusion partner toolchest for the stabilization and crystallization of G protein-coupled receptors. Structure 20, 967–976.

[9] Serrano-Vega, M. J., Magnani, F., Shibata, Y., and Tate, C. G. (2008) Conformational thermostabilization of the β_1-adrenergic receptor in a detergent-resistant form. Proc. Natl. Acad. Sci. U S A 105, 877–882.

[10] Standfuss, J., Edwards, P. C., D'Antona, A., Fransen, M., Xie, G., et al. (2011) The structural basis of agonist-induced activation in constitutively active rhodopsin. Nature 471, 656–660.

[11] Ring, A. M., Manglik, A., Kruse, A. C., Enos, M. D., Weis, W. I., et al. (2013) Adrenaline-activated structure of β_2-adrenoceptor stabilized by an engineered nanobody. Nature 502, 575–579.

[12] Zhang, X., Stevens, R. C., and Xu, F. (2015) The importance of ligands for G protein-coupled receptor stability. Trends Biochem. Sci. 40, 79–87.

[13] Landau, E. M., and Rosenbusch, J. P. (1996) Lipidic cubic phases: a novel concept for the crystallization of membrane proteins. Proc. Natl. Acad. Sci. U S A 93, 14532–14535.

[14] Liu, W., Wacker, D., Gati, C., Han, G. W., James, D., et al. (2013) Serial femtosecond crystallography of G protein-coupled receptors. Science 342, 1521–1524.

[15] Rasmussen, S. G., DeVree, B. T., Zou, Y., Kruse, A. C., Chung, K. Y., et al. (2011) Crystal structure of the β_2 adrenergic receptor-Gs protein complex. Nature 477, 549–555.

[16] Kruse, A. C., Ring, A. M., Manglik, A., Hu, J., Hu, K., et al. (2013) Activation and allosteric modulation of a muscarinic acetylcholine receptor. Nature 504, 101–106.

[17] Huang, W., Manglik, A., Venkatakrishnan, A. J., Laeremans, T., Feinberg, E. N., et al. (2015) Structural insights into μ-opioid receptor activation. Nature 524, 315–321.

[18] Zhang, J., Zhang, K., Gao, Z. G., Paoletta, S., Zhang, D., et al. (2014) Agonist-bound structure of the human $P2Y_{12}$ receptor. Nature 509, 119–122.

[19] Tan, Q., Zhu, Y., Li, J., Chen, Z., Han, G. W., et al. (2013) Structure of the CCR5 chemokine receptor-HIV entry inhibitor maraviroc complex. Science 341, 1387–1390.

[20] Hollenstein, K., Kean, J., Bortolato, A., Cheng, R. K., Dore, A. S., et al. (2013) Structure of class B GPCR corticotropin-releasing factor receptor 1. Nature 499, 438–443.

[21] Zhang, D., Gao, Z. G., Zhang, K., Kiselev, E., Crane, S., et al. (2015) Two disparate ligand-binding sites in the human $P2Y_1$ receptor. Nature 520, 317–321.

[22] Jazayeri, A., Dore, A. S., Lamb, D., Krishnamurthy, H., Southall, S. M., et al. (2016) Extra-helical binding site of a glucagon receptor antagonist. Nature 533, 274–277.

[23] Keov, P., Sexton, P. M., and Christopoulos, A. (2011) Allosteric modulation of G protein-coupled receptors: a pharmacological perspective. Neuropharmacology 60, 24–35.

[24] Fenalti, G., Giguere, P. M., Katritch, V., Huang, X. P., Thompson, A. A., et al. (2014) Molecular control of δ-opioid receptor signalling. Nature 506, 191–196.

[25] Kuwasako, K., Kitamura, K., Nagata, S., Hikosaka, T., and Kato, J. (2011) Structure-function analysis of helix 8 of human calcitonin receptor-like receptor within the adrenomedullin 1 receptor. Peptides 32, 144–149.

[26] Wess, J., Han, S. J., Kim, S. K., Jacobson, K. A., and Li, J. H. (2008) Conformational changes involved in G-protein-coupled-receptor activation. Trends Pharmacol. Sci. 29, 616–625.

[27] Kang, Y., Zhou, X. E., Gao, X., He, Y., Liu, W., et al. (2015) Crystal structure of rhodopsin bound to arrestin by femtosecond X-ray laser. Nature 523, 561–567.
[28] Zhang, K., Zhang, J., Gao, Z. G., Zhang, D., Zhu, L., et al. (2014) Structure of the human $P2Y_{12}$ receptor in complex with an antithrombotic drug. Nature 509, 115–118.
[29] Scholten, D. J., Canals, M., Maussang, D., Roumen, L., and Smit, M. J. (2012) Pharmacological modulation of chemokine receptor function. Br. J. Pharmacol. 165, 1617–1643.
[30] Berger, E. A., Murphy, P. M., and Farber, J. M. (1999) Chemokine receptors as HIV-1 coreceptors: roles in viral entry, tropism, and disease. Annu. Rev. Immunol. 17, 657–700.
[31] Wu, B., Chien, E. Y., Mol, C. D., Fenalti, G., Liu, W., et al. (2010) Structures of the CXCR4 chemokine GPCR with small-molecule and cyclic peptide antagonists. Science 330, 1066–1071.
[32] Warne, T., Serrano-Vega, M. J., Baker, J. G., Moukhametzianov, R., Edwards, P. C., et al. (2008) Structure of a β_1-adrenergic G-protein-coupled receptor. Nature 454, 486–491.
[33] Rasmussen, S. G., Choi, H. J., Fung, J. J., Pardon, E., Casarosa, P., et al. (2011) Structure of a nanobody-stabilized active state of the β_2 adrenoceptor. Nature 469, 175–180.
[34] Xu, F., Wu, H., Katritch, V., Han, G. W., Jacobson, K. A., et al. (2011) Structure of an agonist-bound human A_{2A} adenosine receptor. Science 332, 322–327.
[35] Kroeze, W. K., Sheffler, D. J., and Roth, B. L. (2003) G-protein-coupled receptors at a glance. J. Cell Sci. 116, 4867–4869.
[36] Takakura, H., Hattori, M., Tanaka, M., and Ozawa, T. (2015) Cell-based assays and animal models for GPCR drug screening. Methods Mol. Biol. 1272, 257–270.
[37] Shoichet, B. K., and Kobilka, B. K. (2012) Structure-based drug screening for G-protein-coupled receptors. Trends Pharmacol. Sci. 33, 268–272.
[38] Kumari, P., Ghosh, E., and Shukla, A. K. (2015) Emerging Approaches to GPCR Ligand Screening for Drug Discovery. Trends Mol. Med. 21, 687–701.
[39] Mysinger, M. M., Weiss, D. R., Ziarek, J. J., Gravel, S., Doak, A. K., et al. (2012) Structure-based ligand discovery for the protein-protein interface of chemokine receptor CXCR4. Proc. Natl. Acad. Sci. U S A 109, 5517–5522.
[40] Kolb, P., Rosenbaum, D. M., Irwin, J. J., Fung, J. J., Kobilka, B. K., et al. (2009) Structure-based discovery of β_2-adrenergic receptor ligands. Proc. Natl. Acad. Sci. U S A 106, 6843–6848.
[41] Katritch, V., Jaakola, V. P., Lane, J. R., Lin, J., Ijzerman, A. P., et al. (2010) Structure-based discovery of novel chemotypes for adenosine A_{2A} receptor antagonists. J. Med. Chem. 53, 1799–1809.
[42] de Graaf, C., Kooistra, A. J., Vischer, H. F., Katritch, V., Kuijer, M., et al. (2011) Crystal structure-based virtual screening for fragment-like ligands of the human histamine H_1 receptor. J. Med. Chem. 54, 8195–8206.
[43] Vass, M., Schmidt, E., Horti, F., and Keseru, G. M. (2014) Virtual fragment screening on GPCRs: a case study on dopamine D3 and histamine H4 receptors. Eur. J. Med. Chem. 77, 38–46.
[44] Kruse, A. C., Weiss, D. R., Rossi, M., Hu, J., Hu, K., et al. (2013) Muscarinic receptors as model targets and antitargets for structure-based ligand discovery. Mol. Pharmacol. 84, 528–540.
[45] Rodriguez, D., Brea, J., Loza, M. I., and Carlsson, J. (2014) Structure-based discovery of selective serotonin 5-HT_{1B} receptor ligands. Structure 22, 1140–1151.
[46] Gonzalez-Maeso, J. (2011) GPCR oligomers in pharmacology and signaling. Mol. Brain 4, 20.
[47] Gao, Z. G., and Jacobson, K. A. (2013) Allosteric modulation and functional selectivity of G protein-coupled receptors. Drug Discov. Today Technol. 10, 237–243.
[48] Wisler, J. W., Xiao, K., Thomsen, A. R., and Lefkowitz, R. J. (2014) Recent developments in biased agonism. Curr. Opin. Cell Biol. 27, 18–24.
[49] Palczewski, K., Kumasaka, T., Hori, T., Behnke, C. A., Motoshima, H., et al. (2000) Crystal Structure of Rhodopsin: A G Protein-Coupled Receptor. Science 289, 739–745.
[50] Murakami, M., and Kouyama, T. (2008) Crystal structure of squid rhodopsin. Nature 453, 363–367.
[51] Cherezov, V., Rosenbaum, D. M., Hanson, M. A., Rasmussen, S. G., Thian, F. S., et al. (2007) High-resolution crystal structure of an engineered human β_2-adrenergic G protein-coupled receptor. Science 318, 1258–1265.
[52] Warne, T., Edwards, P. C., Leslie, A. G., and Tate, C. G. (2012) Crystal structures of a stabilized β_1-adrenoceptor bound to the biased agonists bucindolol and carvedilol. Structure 20, 841–849.
[53] Shimamura, T., Shiroishi, M., Weyand, S., Tsujimoto, H., Winter, G., et al. (2011) Structure of the human histamine H_1 receptor complex with doxepin. Nature 475, 65–70.
[54] Chien, E. Y., Liu, W., Zhao, Q., Katritch, V., Han, G. W., et al. (2010) Structure of the human dopamine D3 receptor in complex with a D2/D3 selective antagonist. Science 330, 1091–1095.
[55] Wang, C., Jiang, Y., Ma, J., Wu, H., Wacker, D., et al. (2013) Structural basis for molecular recognition at serotonin receptors. Science 340, 610–614.
[56] Wacker, D., Wang, C., Katritch, V., Han, G. W., Huang, X., et al. (2013) Structural features for functional selectivity at serotonin receptors. Science 340, 615–619.
[57] Thal, D. M., Sun, B., Feng, D., Nawaratne, V., Leach, K., et al. (2016) Crystal structures of the M1 and M4 muscarinic acetylcholine receptors. Nature 531, 335–340.
[58] Haga, K., Kruse, A. C., Asada, H., Yurugi-Kobayashi, T., Shiroishi, M., et al. (2012) Structure of the human M2 muscarinic acetylcholine receptor bound to an antagonist. Nature 482, 547–551.
[59] Kruse, A. C., Hu, J., Pan, A. C., Arlow, D. H., Rosenbaum, D. M., et al. (2012) Structure and dynamics of the M3 muscarinic acetylcholine receptor. Nature 482, 552–556.
[60] Jaakola, V. P., Griffith, M. T., Hanson, M. A., Cherezov, V., Chien, E. Y., et al. (2008) The 2.6 angstrom crystal structure of a human A_{2A} adenosine receptor bound to an antagonist. Science 322, 1211–1217.
[61] Lebon, G., Warne, T., Edwards, P. C., Bennett, K., Langmead, C. J., et al. (2011) Agonist-bound adenosine A_{2A} receptor structures reveal common features of GPCR activation. Nature 474, 521–525.
[62] Qin, L., Kufareva, I., Holden, L. G., Wang, C., Zheng, Y., et al. (2015) Crystal structure of the chemokine receptor CXCR4 in complex with a viral chemokine. Science 347, 1117–1122.
[63] Thompson, A. A., Liu, W., Chun, E., Katritch, V., Wu, H., et al. (2012) Structure of the nociceptin/orphanin FQ receptor in complex with a peptide mimetic. Nature 485, 395–399.
[64] Wu, H., Wacker, D., Mileni, M., Katritch, V., Han, G. W., et al. (2012) Structure of the human κ-opioid receptor in complex with JDTic. Nature 485, 327–332.
[65] Manglik, A., Kruse, A. C., Kobilka, T. S., Thian, F. S., Mathiesen, J. M., et al. (2012) Crystal structure of the μ-opioid receptor bound to a morphinan antagonist. Nature 485, 321–326.
[66] White, J. F., Noinaj, N., Shibata, Y., Love, J., Kloss, B., et al. (2012) Structure of the agonist-bound neurotensin receptor. Nature 490, 508–513.
[67] Zhang, C., Srinivasan, Y., Arlow, D. H., Fung, J. J., Palmer, D., et al. (2012) High-resolution crystal structure of human protease-activated receptor 1. Nature 492, 387–392.
[68] Yin, J., Mobarec, J. C., Kolb, P., and Rosenbaum, D. M. (2015) Crystal structure of the human OX_2 orexin receptor bound to the insomnia drug suvorexant. Nature 519, 247–250.
[69] Zhang, H., Unal, H., Gati, C., Han, G. W., Liu, W., et al. (2015) Structure of the Angiotensin receptor revealed by serial femtosecond crystallography. Cell 161, 833–844.
[70] Hanson, M. A., Roth, C. B., Jo, E., Griffith, M. T., Scott, F. L., et al. (2012) Crystal structure of a lipid G protein-coupled receptor. Science 335, 851–855.
[71] Srivastava, A., Yano, J., Hirozane, Y., Kefala, G., Gruswitz, F., et al. (2014) High-resolution structure of the human GPR40 receptor bound to allosteric agonist TAK-875. Nature 513, 124–127.
[72] Chrencik, J. E., Roth, C. B., Terakado, M., Kurata, H., Omi, R., et al. (2015) Crystal Structure of Antagonist Bound Human Lysophosphatidic Acid Receptor 1. Cell 161, 1633–1643.

[73] Siu, F. Y., He, M., de Graaf, C., Han, G. W., Yang, D., et al. (2013) Structure of the human glucagon class B G-protein-coupled receptor. Nature 499, 444–449.
[74] Wu, H., Wang, C., Gregory, K. J., Han, G. W., Cho, H. P., et al. (2014) Structure of a class C GPCR metabotropic glutamate receptor 1 bound to an allosteric modulator. Science 344, 58–64.
[75] Dore, A. S., Okrasa, K., Patel, J. C., Serrano-Vega, M., Bennett, K., et al. (2014) Structure of class C GPCR metabotropic glutamate receptor 5 transmembrane domain. Nature 511, 557–562.
[76] Wang, C., Wu, H., Katritch, V., Han, G. W., Huang, X., et al. (2013) Structure of the human smoothened receptor bound to an antitumour agent. Nature 497, 338–343.